Stress and growth of Ag monolayers on a Fe(100) whisker

R. Mahesh, D. Sander,* S. M. Zharkov,† and J. Kirschner
Max-Planck-Institut für Mikrostrukturphysik, Weinberg 2, D-06120 Halle, Germany
(Received 3 December 2002; revised manuscript received 21 February 2003; published 17 July 2003)

In situ stress measurements have been performed during the deposition of epitaxial Ag monolayers on a Fe whisker. A compressive stress of -0.6 GPa is measured above a 5-ML Ag thickness which is ascribed to the epitaxial misfit of -0.8% between Ag and Fe. Back-extrapolation of the coverage dependent stress measurements to zero coverage reveals an Ag-induced change of the surface stress of Fe(100) of -1.23 N/m. Comparing this surface stress change with the calculated surface stress for Ag(100) suggests a tensile surface stress of $+2.05$ N/m for clean Fe(100). The deposition of 2–5 layers of Ag does not change the stress induced by the first layer significantly. This almost stress free growth is assigned to a rougher surface morphology which is most likely caused by a surface alloy formation.

DOI: 10.1103/PhysRevB.68.045416 PACS number(s): 68.35.Ct, 68.35.Gy, 68.55.Jk, 68.60.Bs

I. INTRODUCTION

The interesting magnetic properties of multilayer structures[1–4] as compared to bulk elements have induced considerable work in this field. One example is the magnetic exchange coupling between ferromagnetic layers, which is mediated by the nonferromagnetic spacer layer.[5–13]

The growth of Ag on Fe(100) is a prototype for modified magnetic and electronic properties of layered structures. The exchange coupling between Fe layers separated by an Ag spacer has been studied extensively,[14–16] and electronic quantum well states have been observed for epitaxial Ag films deposited on Fe(100).[17–21] Sharp interfaces and flat films are mandatory for the study of interlayer exchange coupling and quantum wells, and the growth of Ag on Fe seems to satisfy the structural and thermodynamic criteria expected for a perfect layer-by-layer growth (Frank–van der Merwe growth mode). The lattice mismatch η between fcc Ag(100) and bcc Fe(100) is small, $\eta=-0.008$, and this suggests that the elastic energy of the epitaxially strained film will be of only minor importance for the resulting growth mode as compared to kinetic arguments. The lower surface free energy γ of Ag(100), (1.2 J/m^2) (Ref. 22) in comparison to Fe(100), (2.2 J/m^2) (Ref. 22) also favors the wetting of Fe(100) surface by Ag.

In spite of the seemingly favorable conditions for layer-by-layer growth, previous work by other groups indicated a subtle interplay between the growth parameters such as deposition rate and sample temperature which have to be adjusted properly to ensure the growth of flat Ag films.[18,14,19–21]

The goal of the present investigation is to correlate film stress with the growth mode of Ag on Fe(100). Our direct measurement of film stress by the curvature technique reveals that different growth regimes can be clearly identified by the characteristic stress behavior. For layer-by-layer growth a compressive film stress of -0.6 GPa is found in Ag films thicker than five layers, which corresponds to the misfit stress as calculated from Ag bulk elasticity. The deposition of one layer Ag on Fe(100) relieves the tensile surface stress of Fe. We conclude from an extrapolation of our stress measurements to zero coverage that the surface stress of clean Fe(100) along [100] is of the order of 2 N/m. Our stress measurements identify a nearly constant surface stress with increasing Ag thickness between 2–5-ML Ag deposition (1-ML Ag: 2.043 Å), before misfit stress sets in for large film thickness. We ascribe the absence of misfit stress to a possible surface alloy formation between Ag and Fe .

II. EXPERIMENT

We use Fe(100) whiskers which were grown by gas phase epitaxy.[23] The needlelike whiskers with a length (L) of 10 mm have a nearly square cross section of 100×100 μm^2 with (100) surfaces, the long edge runs along [100]. Fe whiskers offer very flat surfaces with terrace sizes of the order of 1 μm; separated by single atom high steps (0.144 nm). The Fe whisker was clamped at one end along its width to a sample manipulator leaving the other end free.

The experiments were performed in an ultra high vacuum chamber with a base pressure of 1×10^{-10} mbar. The whisker was subjected to several Ar^+ ion sputtering (ion energy: 2 keV; sample current: 1 μA, 300 K) and annealing cycles. The Fe whisker was annealed to 1270 K by radiation from a hot tungsten filament mounted behind a tungsten radiation shield, which is placed in between the whisker and the filament. The whisker temperature was monitored using a thermocouple attached to the sample holder close to the whisker. This thermocouple was calibrated against thermocouples which were attached to a test whisker. We estimate the accuracy of our temperature measurement to be ±10 K. After sputtering and annealing, carbon was found by Auger electron spectroscopy (AES) on the whisker, [I(C 271 eV)/I(Fe 703 eV)$=10$ %]. Carbon was removed by mild oxidation at 1×10^{-7} mbar O_2 at 300 K and subsequent annealing to 630 K. This procedure yields a clean Fe surface with O and C surface contamination below the detection limits of AES (approximately 1 at. %). Low energy eletron diffraction patterns of the clean Fe(100) whisker thus obtained showed sharp 1×1 diffraction spots.

High purity Ag (ADVENT, 99.99%) (Ref. 24) was evaporated from a electron-beam heated molybdenum crucible onto the Fe(100) whisker at deposition rates between 0.006

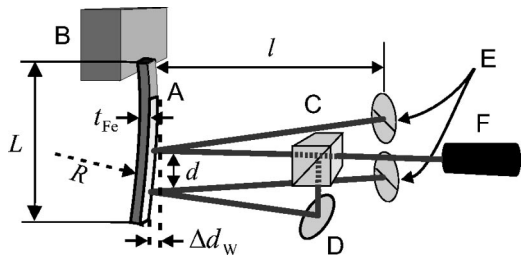

FIG. 1. Schematic representation of the two beam optical deflection set up to measure the stress-induced whisker curvature. (A) Fe whisker, (B) manipulator, (C) beam splitter, (D) mirror, (E) position sensitive detectors, and (F) laser. L: length of whisker; t_{Fe}: thickness of whisker; R: radius of whisker curvature; Δd_w: deflection of bottom end of the whisker, d: spot separation; l: whisker-detector distance.

and 0.8 Å/s and whisker temperatures between 175 and 393 K. The growth rates were calibrated before and after each stress measurement by a quartz crystal oscillator. One ML of Ag corresponds to a 2.043-Å-thick film with an areal density of 1.2×10^{15} atoms/cm^2. The thermal stability at low and high temperatures was generally better than ±0.05 K/min. The residual gas pressure during evaporation remained below 5×10^{-10} mbar.

Ag-induced surface stress is measured by a highly sensitive optical beam deflection technique, which is schematically shown in Fig. 1. Two laser beams are reflected from two points vertically displaced on the surface of the whisker by d (approximately 5 mm) onto two position-sensitive split-photodiode detectors, which are mounted at a distance l away from the whisker. The difference of the position signals of the two detectors is directly proportional to the substrate curvature $1/R$, where R is the radius of curvature of the substrate. One benefit of the two beam optical method is the direct determination of the curvature change $\Delta(1/R)=(\Delta Pos1-\Delta Pos2)/(2ld)$, where the laser spot deflections on the detectors are given by $\Delta Pos1$,$\Delta Pos2$. The conversion of the position signal of the split photodetector into a spot deflection is accomplished by moving the detectors by a known distance with a calibrated piezo drive and noting the resulting change of the position signal. From the measured change of curvature $\Delta(1/R)$ the corresponding change of film thickness integrated stress $\Delta(\tau_{Ag}\, t_{Ag})$ is calculated. In the limit of submonolayer Ag coverage, this stress corresponds to the Ag-induced change of surface stress of the Fe substrate $\Delta(\tau_{Fe}^{(S)})$:

$$\Delta(\tau_{Fe}^{(S)})=\Delta(\tau_{Ag}\, t_{Ag})=\frac{Yt_{Fe}^2}{6(1-\nu)}\;\Delta\frac{1}{R}, \qquad (1)$$

where Y is the Young's modulus of Fe(100), ν is the Poisson ratio, and t_{Fe} (100 μm) is the thickness of the Fe whisker.[25–27] Numerical values are given in Table I. The stress-induced deflections of the whisker are small. A coverage of 1-ML Ag induces a surface stress change of -2 N/m at 300 K, which leads to a radius of curvature R of 140 m, and the bottom end of the whisker (Δd_w) is displaced by 0.36 μm.

TABLE I. Elastic compliance constants s_{ij}, Young's modulus $Y_{(100)}$, and Poisson ratio ν of Ag and Fe.

Element	s_{11} $(\mathrm{TPa})^{-1}$	s_{12} $(\mathrm{TPa})^{-1}$	$Y_{(100)}=1/s_{11}$ (GPa)	$\nu=-s_{12}/s_{11}$
fcc Ag	22.9[a]	-9.80[a]	43.67	0.423
bcc Fe	7.64[a]	-2.81[a]	130.89	0.368

[a]Ref. 42.

III. MISFIT STRESS OF AG ON FE

The epitaxial relation between fcc Ag [$a_{Ag}=4.08$ Å (Ref. 28)] and bcc Fe [$a_{Fe}=2.866$ Å (Ref. 28)] is described by 45° rotated unit cells of the two elements. This leads to a small compressive in-plane lattice misfit $\eta=(a_{Fe}-a_{Ag}/\sqrt{2})/(a_{Ag}/\sqrt{2})=-0.8\%$. From this we calculate a biaxial film stress of $\tau=\eta Y_{Ag}/(1-\nu_{Ag})=-0.61$ GPa. Our stress measurements presented below confirm this magnitude of stress for layer-by-layer growth conditions for $t_{Ag}>5$ ML. Thus, bulk elasticity is applicable under these conditions, and we derive an elastic energy per Ag atom of $F_{el}=\tau\ \eta=0.5$ meV. This elastic energy contribution is one to two orders of magnitude smaller compared to epitaxial systems like Co/Cu(100) ($\eta=1.7\%;\tau=3.23$ GPa) (Ref. 29) or Fe/W(100) ($\eta=10.1\%;\tau=21$ GPa).[26] Consequently, and in contrast to these former studies, we expect for the growth of Ag on Fe that growth kinetics are more decisive for the resulting growth mode than lattice misfit considerations.

The different step heights of fcc-Ag(100)(2.05 Å) and bcc Fe(100)(1.44 Å) induce a considerable vertical misfit of 42%. This vertical misfit is expected to induce distortions in the Ag film at step edges of the substrate. However, in a simplified model of Ag growth we neglect the possible impact of the vertical distortion on the in-plane misfit stress. This simplification seems justified for thicker films where a close agreement between theory and experiment is found for the in-plane stress. In the monolayer range however, the atomic size mismatch between Ag and Fe could be a decisive driving force for interface alloying, as discussed below.

IV. STRESS MEASUREMENTS DURING AG DEPOSITION

Stress measurements were carried out during growth at deposition rates between 0.006 and 0.8 Å/s and sample temperatures ranging from 300 to 393 K. We find that the general features of the stress signal τt_{Ag} as a function of Ag film thickness t_{Ag} are similar in this range of temperature and deposition rate.

A typical stress measurement is shown in Fig. 2. As the shutter of the Ag evaporator is opened, we find a large compressive stress of -2 N/m until 1 ML has been deposited. We call this stress regime I, and we ascribe the measured stress to the Ag-induced change of the surface stress of Fe(100). With increasing coverage we observe a slight increase of the stress signal in regime II, before the stress signal decreases monotonically in regime III for $t_{Ag}>5$ ML. Stress regime III is ascribed to the misfit induced stress. These stress regimes are found for all experiments performed in this temperature range.

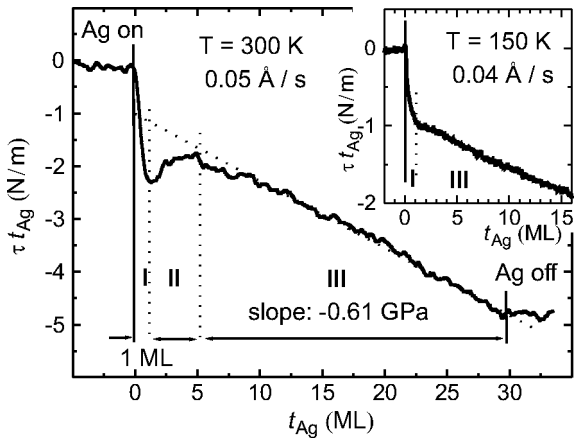

FIG. 2. A typical plot of stress as a function of thickness showing the three distinct stress regimes during the growth of Ag on a Fe(100) whisker. Regimes I, II and III correspond to the initial surface stress change, transition of the growth mode, and regular misfit stress, respectively. The inset shows a stress measurement at 150 K, where regime II is absent.

The stress behavior in regime II comes as a surprise, as no structural transitions are expected in this thickness range between 1 and 5 ML. A qualitative inspection of the low energy electron diffraction pattern of Fig. 3 does not reveal any indication of a structural change between a clean Fe(100) surface (regime I) in (a) and a 6-ML Ag coverage (regime II-III crossover) in (b), except for a slight increase of the diffuse intensity around the center of the diffraction image at the (0,0) position in Fig. 3(b).

A thermally induced experimental artifact for the stress behavior in regime II can be ruled out, as the same thickness dependence of the stress is measured in an interrupted growth experiment. The shutter of the evaporator is closed after deposition of 1-ML Ag. Deposition is resumed after 10 min., and we still measure a stress regime II before detecting regime III at 6 ML. This indicates that regime II does not correspond to a possible thermal relaxation of the whisker-manipulator compound upon exposure to the Ag oven.

Deposition at 150 K leads to the absence of regime II, and a direct transition from the surface stress dominated regime I to regime III is observed. The inset of Fig. 2 shows such a low temperature stress measurement. The stress curve indicates that already for the second layer of Ag the stress regime III is reached.

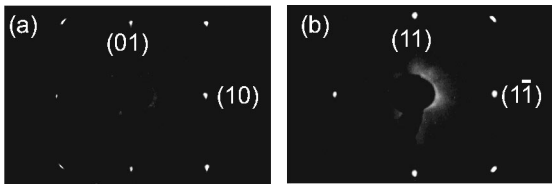

FIG. 3. Low energy electron diffraction (LEED) patterns of (a) a clean Fe (100) whisker, and (b) a 6-ML Ag film on the Fe (100) whisker (corresponding to the stress regime II-III crossover). Similar and sharp diffraction spots with low background intensity in (b) as compared to the clean Fe surface in (a) indicate that the Ag film is epitaxially well ordered, with no indications of a structural transition.

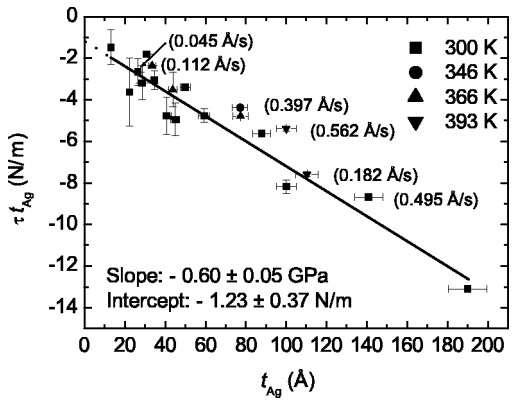

FIG. 4. The total stress change as a function of the thickness of Ag grown on Fe whisker. The back extrapolation gives the Ag-induced surface stress change.

V. DISCUSSION

Our discussion focuses on the correlation between the measurements of film stress and the observation of different growth regimes. The reader is referred to the literature for thermodynamical consideration regarding film growth.[30–32]

Figure 4 summarizes a series of stress measurements at room temperature and above. The total stress change after completion of growth is plotted as a function of the Ag film thickness. The solid line of Fig. 4 is a least square fit to the data points. The fit indicates a slope of -0.6 ± 0.05 GPa and an intercept of -1.23 ± 0.37 N/m. The close agreement between the averaged slope and the calculated value of -0.61 GPa from the lattice misfit confirms our conclusion that the epitaxial misfit stress for $t_{Ag}>5$ ML is well described by continuum elasticity. Consequently, we ascribe regime III to the epitaxial misfit stress in the growing film. This conclusion is supported by the slope of the individual stress curves in regime III, -0.61 GPa, which is within experimental error of $\pm10\%$, in agreement with the calculated misfit stress of -0.61 GPa.

We propose that the intercept of the least square fit line with the stress axis in Fig. 4 can be ascribed to the Ag-induced change of the surface stress of the clean Fe(100) surface. If there was no difference of the surface stress of Fe vs Ag, we would expect a zero intercept, i.e.n an individual curve like the one shown in Fig. 2 should back-extrapolate to the stress of the starting point. This is however not the case. Back-extrapolation leads to a *more negative* stress value. This indicates that the surface stress of clean Fe is larger in magnitude as compared to that of Ag. We are not aware of any calculated values of surface stress for Fe,[22] but for Ag(100) $\tau^{(S)}_{100}[\mathrm{Ag}]=0.82$ N/m has been calculated.[33] We assume that the surface stress change of -1.23 ± 0.37 N/m, as obtained by back-extrapolation of the measured surface stress to zero coverage, is given by difference of surface stress between Fe and Ag. From this we deduce $\tau^{(S)}_{100}[\mathrm{Fe}]=2.05$ N/m as the surface stress of Fe(100) along [100].

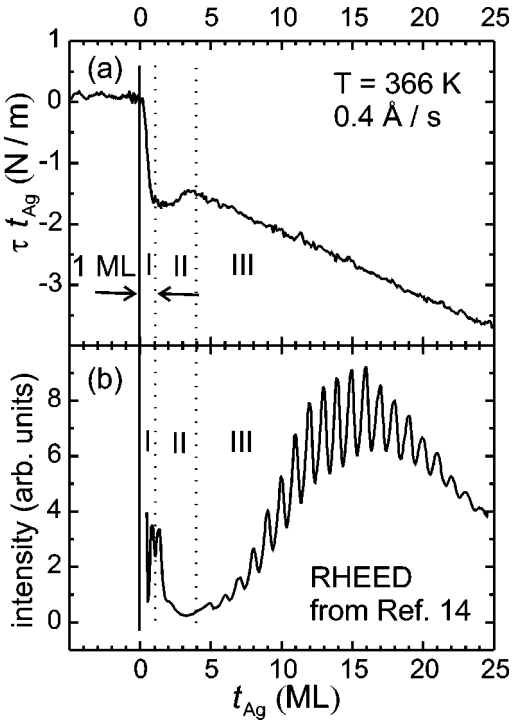

FIG. 5. Comparison of the stress data (a) with RHEED investigations (adapted from Ref. 14 with the kind permission of the authors) during the growth of Ag on a Fe whisker under similar high temperature growth conditions. (b) Pronounced RHEED oscillations due to layer-by-layer growth are seen in the misfit stress regime III while they are absent in regime II.

Whereas surface stress and epitaxial misfit stress are clearly responsible for the measured stress in regimes I and III, respectively, the intermediate regime II is unexpected. We discuss its physical origin in connection with the observation of an ''incubation'' period in the reflection high energy electron diffraction (RHEED) intensity oscillation measurements by Unguris *et al.*.[14] Fe whiskers were also used in their growth and magnetism study,[14] and we are therefore confident that our stress results which were obtained under similar growth conditions reflect the same surface morphology as their RHEED study.

In Fig. 5 we compare (a) our stress measurements taken under comparable conditions as the RHEED data by Unguris *et al.* shown in (b). We added our labels I, II and III to their data in (b) and we find that regime II is characterized by the absence of RHEED intensity oscillations. Evenly spaced RHEED oscillations become stronger as the system enters regime III. Unguris *et al.*[14] attributed the absence of the RHEED intensity oscillations to disorder and roughness of the Ag film for this thickness range between 1–5 ML.

It seems plausible to ascribe the absence of RHEED oscillations and the peculiar stress behavior in regime II to the same origin. This assertion is corroborated by stress measurements, which we performed at a lower temperature of 150 K and by RHEED measurements by Heinrich *et al.*[15] at 140 K. We did not observe a stress regime II for this low temperature growth, as can be seen in the inset of Fig. 2. Instead, we measured a monotonic compressive stress which followed directly the initial stress change in region I, i.e., regime III of Fig. 5(a) directly follows regime I. The low temperature RHEED data of Heinrich *et al.* show intensity oscillations in the whole thickness range, in contrast to the absence of oscillations for the 366 K measurements shown in Fig. 5(b). We conclude that both stress and RHEED measurements indicate a change of the growth mode at lower temperature.

We suggest that the larger tendency for surface alloy formation at higher temperature could be an important aspect of the temperature-driven change of growth mode. If one assumes some intermixing between Ag and Fe at 366 K, this will lead to an interface region, which is chemically inhomogeneous and also structurally distorted due to the larger atomic size of Ag as compared to Fe. The intermixing of the surface region renders an estimate of the misfit between the deposit and the substrate doubtful, as we have no information on the chemical composition of a potential surface alloy, nor on its spatial homogeneity. Assuming substitutional diffusion of Ag into the Fe surface, we expect that Fe will be expelled and subsequently incorporated into the growing Ag film. The amount of intermixing, i.e., the atomic concentration of Fe within the Ag deposit will be smaller with increasing Ag thickness. This offers an explanation as to why the system reverts to the regular stress and RHEED behavior for larger Ag thickness in regime III. Intermixing is thermally activated,[34–39] and leads to negligible intermixing at low temperature. This explains the different stress and RHEED behavior at low temperature as compared to deposition at higher temperature.

This explanation relies on surface alloy formation of Ag in Fe. Although Ag is not miscible in bulk Fe,[40] surface alloy formation is a well documented general phenomenon.[41] In short, atomic size mismatch suppresses intermixing in the bulk, but it favors intermixing at the surface. A recent scanning tunneling microscopy study of Au growth on a Fe(100) whisker identified surface alloy formation for this chemically and structurally similar system (Ag and Au have a nearly identical atomic volume).[39] Therefore we expect some tendency for surface alloy formation also for Ag on Fe, though we are not aware of any experimental study which might offer direct experimental evidence for surface alloy formation of this system.

VI. CONCLUSION

Stress measurements are a sensitive tool to identify different growth regimes in monolayer thin films. A comparison between measured stress and calculated misfit stress suggests that the growth of Ag on Fe occurs in the layer-by-layer mode for films thicker than five layers. The measured stress of -0.6 GPa in this regime corresponds to the calculated misfit stress, and indicates the applicability of continuum elasticity for films as thin as 1 nm. The back-extrapolation to zero coverage indicates a surface stress of clean Fe(100) of 2.05 N/m, which is reduced upon Ag deposition. We ascribe the unexpected intermediate stress regime II at 1–5-ML Ag to a possible surface alloy formation. We performed stress

measurements at a low temperature (150 K), which did not show the intermediate stress regime II. Instead, the stress curve proceeds directly from regime I to regime III. These results together with earlier RHEED work by other groups support our conclusion that changes of the growth mode can be traced with high sensitivity by in situ stress measurements and suggest that regime II is due to alloy formation between Fe and Ag.

ACKNOWLEDGMENTS

We thank H.Menge for the skillful preparation of high quality Fe whiskers.

*Corresponding author. Email address: sander@mpi-halle.de. FAX: ++49-345-5511-223

†Permanent address: L. V. Kirensky Institute of Physics of Russian Academy of Sciences, Krasnoyarsk, 660036, Russia. Email address: zharkov@iph.krasn.ru

[1] P. Grünberg, R. Schreiber, Y. Pang, M.B. Brodsky, and H. Sowers, Phys. Rev. Lett. **57**, 2442 (1986).

[2] M.N. Baibich, J.M. Broto, A. Fert, F.N. Van Dau, F. Petroff, P. Etienne, G. Creuzet, A. Friederich, and J. Chazelas, Phys. Rev. Lett. **61**, 2472 (1988).

[3] C. Carbone and S.F. Alvarado, Phys. Rev. B **36**, 2433 (1987).

[4] L.M. Falicov, Phys. Today **45**, 46 (1992).

[5] S.S.P. Parkin, N. More, and K.P. Roche, Phys. Rev. Lett. **64**, 2304 (1990).

[6] P. Bruno and C. Chappert, Phys. Rev. Lett. **67**, 1602 (1991).

[7] S.T. Purcell, W. Folkerts, M.T. Johnson, N.W.E. McGee, K. Jager, J. aan de Stegge, W.B. Zeper, W. Hoving, and P. Grünberg, Phys. Rev. Lett. **67**, 903 (1991).

[8] J. Unguris, R.J. Celotta, and D.T. Pierce, Phys. Rev. Lett. **67**, 140 (1991).

[9] Z. Celinski and B. Heinrich, J. Magn. Magn. Mater. **99**, L25 (1991).

[10] M.E. Brubaker, J.E. Mattson, C.H. Sowers, and S.D. Bader, Appl. Phys. Lett. **58**, 2306 (1991).

[11] Z.Q. Qiu, J. Pearson, and S.D. Bader, Phys. Rev. B **46**, 8659 (1992).

[12] M.D. Stiles, Phys. Rev. B **48**, 7238 (1993).

[13] P. Bruno, in *Magnetism: Molecules to Materials III, Nanosized Magnetic Materials*, edited by Joel S. Miller and Marc Drillon (Wiley-VCH, Weinheim, 2002).

[14] J. Unguris, R.J. Celotta, and D.T. Pierce, J. Magn. Magn. Mater. **127**, 205 (1993).

[15] B. Heinrich, K.B. Urquhart, J.R. Dutcher, S.T. Purcell, J.F. Cochran, A.S. Arrott, D.A. Steigerwald, and W.F. Egelhoff, Jr., J. Appl. Phys. **63**, 3863 (1988).

[16] A. Fuß, S. Demorkritov, P. Grünberg, and W. Zinn, J. Magn. Magn. Mater. **103**, L221 (1992).

[17] J.J. Paggel, T. Miller, and T.-C. Chiang, Phys. Rev. Lett. **83**, 1415 (1999).

[18] N.B. Brookes, Y. Chang, and P.D. Johnson, Phys. Rev. B **50**, 15 330 (1994).

[19] J.J. Paggel, T. Miller, and T.-C. Chiang, J. Electron Spectrosc. Relat. Phenom. **101-103**, 271 (1999).

[20] S. Ogawa, H. Nagano, and H. Petek, Phys. Rev. Lett. **88**, 116801 (2002).

[21] S. De Rossi, A. Tagliaferri, and F. Ciccacci, J. Magn. Magn. Mater. **157–158**, 287 (1996).

[22] D. Sander and H. Ibach, in *Physics of Covered Solid Surfaces*, edited by H.P. Bonzel, Landolt-Börnstein, New Series, Group III, Vol. 42, Pt. A2 (Springer-Verlag, Berlin, 2002), Chap. 4.4-1.4-49.

[23] H. Menge (private communication).

[24] ADVENT Research Materials Ltd, Oxford, U.K., www.advent-rm.com.

[25] H. Ibach, Surf. Sci. Rep. **29**, 193 (1997).

[26] D. Sander, Rep. Prog. Phys. **62**, 809 (1999).

[27] K. Dahmen, S. Lehwald, and H. Ibach, Surf. Sci. **446**, 161 (2000).

[28] Powder Diffraction File, JCPDS International Center for Diffraction Data, Swarthmore, PA, USA, Inorganic, card numbers: 04-0783 (Ag), 06-0696 (Fe).

[29] D. Sander, S. Ouazi, V.S. Stepanyuk, D.I. Bazhanov, and J. Kirschner, Surf. Sci. **512**, 281 (2002).

[30] R. Kern, G. Le Lay, and J.J. Metois, in *Current Topics in Materials Science*, edited by E. Kaldis (Amsterdam, North-Holland, 1979), Vol. 3.

[31] S. Stoyanov and D. Kashiev, in *Current Topics in Materials Science*, edited by E. Kaldis (North-Holland, Amsterdam, 1981), Vol. 7.

[32] J.A. Venables, G.D.T. Spiller, and M. Hanbücken, Rep. Prog. Phys. **47**, 399 (1984).

[33] P. Gumbsch and M.S. Daw, Phys. Rev. B **44**, 3934 (1991).

[34] D.A. Steigerwald, I. Jacob, and J.W.F. Egelhoff, Surf. Sci. **202**, 472 (1988).

[35] W. Daum, C. Stuhlmann, and H. Ibach, Phys. Rev. Lett. **26**, 2741 (1988).

[36] H. Glatzel, T. Fauster, B.M.U. Scherzer, and V. Dose, Surf. Sci. **254**, 58 (1991).

[37] S.A. Chambers, T.J. Wagener, and J.H. Weaver, Phys. Rev. B **36**, 8992 (1987).

[38] M. Arnott, E.M. McCash, and W. Allison, Surf. Sci. **269-270**, 724 (1992).

[39] M.M.J. Bischoff, T. Yamada, A.J. Quinn, R.G.P. van der Kraan, and H. van Kempen, Phys. Rev. Lett. **87**, 246102 (2001).

[40] *Binary Alloy Diagrams*, edited by T.B. Massalski (American Society for Metals, Metals Park, OH, 1986).

[41] J. Tersoff, Phys. Rev. Lett. **74**, 434 (1994).

[42] R.F.S. Hearmon, in *The Elastic Constants of Non-Piezoelectric Crystals*, edited by K.H. Hellwege and A.M. Hellwege, Landolt-Börnstein, New Series, Group III, Vol. 2 (Springer-Verlag, Berlin, 1969).